

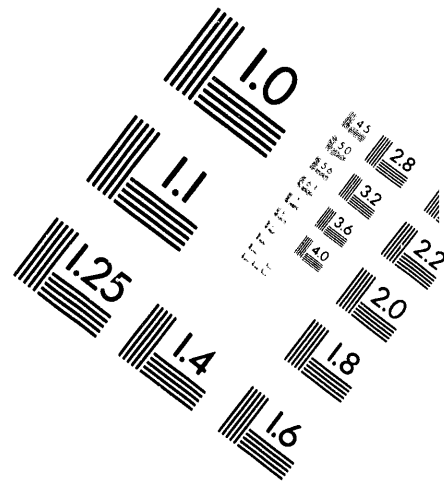
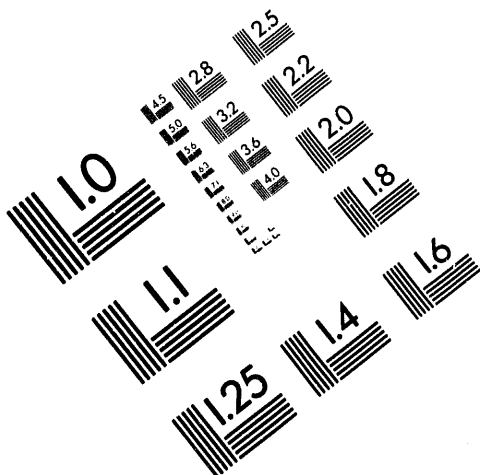


AIM

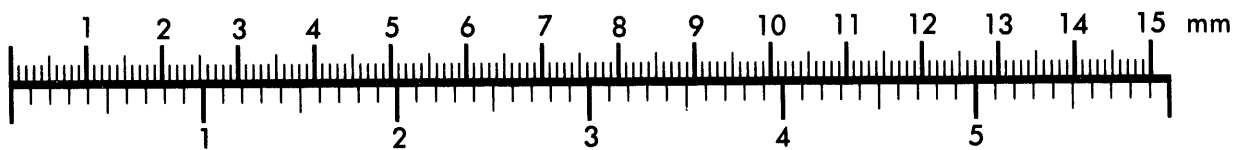
Association for Information and Image Management

1100 Wayne Avenue, Suite 1100
Silver Spring, Maryland 20910

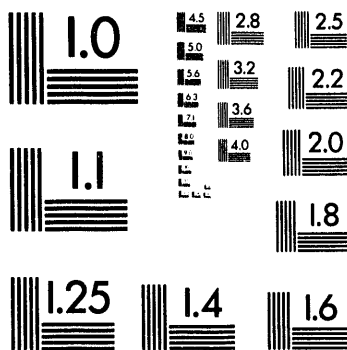
301/587-8202



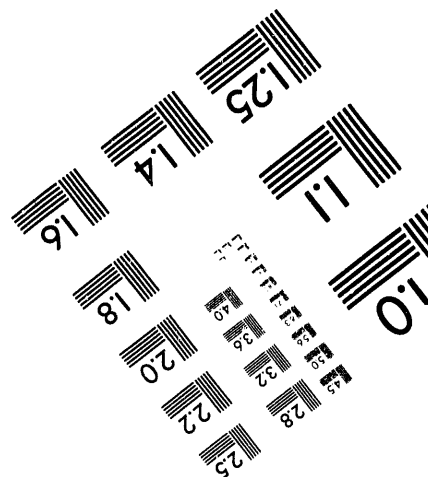
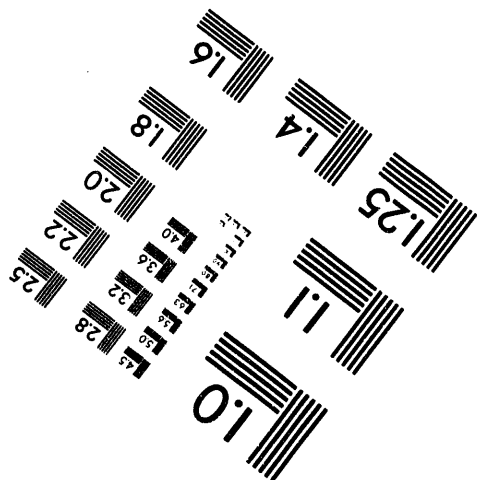
Centimeter



Inches



MANUFACTURED TO AIM STANDARDS
BY APPLIED IMAGE, INC.



1 of 1

DECLASSIFIED

HW-75611
Page 1

This document consists of
36 pages,

This document classified by:

ORIGINAL SIGNED BY
T. W. [REDACTED]

C REACTOR OVERBORE FUEL EXAMINATION

By

K. L. Hladek
Reactor Engineering

R. Teats
Radiometallurgy Laboratory

E. A. Weakley
Quality and Process Control Engineering

April 18, 1963

HANFORD ATOMIC PRODUCTS OPERATION
RICHLAND, WASHINGTON

MASTER

NOTICE

This report was prepared for use within General Electric Company in the course of work under Atomic Energy Commission Contract AT(45-1) - 1350, and any views or opinions expressed in the report are those of the author only. This report is subject to revision upon collection of additional data.

LEGAL NOTICE

This report was prepared as an account of Government sponsored work. Neither the United States, nor the Commission, nor any person acting on behalf of the Commission:

- A. Makes any warranty or representation, expressed or implied, with respect to the accuracy, completeness, or usefulness of the information contained in this report, or that the use of any information, apparatus, method, or process disclosed in this report may not infringe privately owned rights; or
- B. Assumes any liabilities with respect to the use of, or for damages resulting from the use of any information, apparatus, method, or process disclosed in this report.

As used in the above, "person acting on behalf of the Commission" includes any employee or contractor of the Commission, or employee of such contractor, to the extent that such employee or contractor of the Commission, or employee of such contractor prepares, disseminates, or provides access to, any information pursuant to his employment or contract with the Commission, or his employment with such contractor.

DECLASSIFIED

DISTRIBUTION OF THIS DOCUMENT IS UNLIMITED

87B

Classified by [REDACTED]
DECLASSIFIED

By Authority of CG-PR-2,
DS Lewis, 3-15-94
By Jerri Maley, 4-6-94
Verified By J.E. Sawley,
4-15-94

DECLASSIFIED

HW-75611

Page 2

DISTRIBUTION

1. F. W. Albaugh
2. T. W. Ambrose
3. E. R. Astley
4. J. M. Bird
5. W. A. Blanton
6. A. G. Blasewitz
7. R. R. Bloomstrand
8. S. H. Bush
9. J. J. Cadwell
10. M. A. Clinton
11. R. E. Dunn
12. W. J. Ferguson
13. O. H. Greager
14. W. J. Gruber
15. C. M. Heeb
16. K. L. Hladek
17. R. T. Jessen
18. F. W. Knight
19. G. A. Last
20. J. E. Minor
21. W. N. Mobley
22. R. E. Olson
23. R. W. Reid
24. O. C. Schroeder
25. H. G. Spencer
26. J. T. Stringer
27. R. Teats
28. F. W. VanWormer
29. E. E. Voiland
30. E. A. Weakley
31. O. J. Wick
32. S. A. Wood
33. 300 Files
34. Record Center

DECLASSIFIED

HW-75611
Page 3

C REACTOR OVERBORE FUEL EXAMINATION

INTRODUCTION

On April 16, 1962, the fuel charge in overbore tube 3062-C sustained a failure, and upon examination after discharge was found to contain three split failures and three "worm tracked" elements (depression in the aluminum cladding apparently the result of uranium cleavage and subsequent yielding of the cladding). These failures occurred approximately ten days following a period of reactor neutron flux cycling, and during a second cycle at C Reactor. In addition to the failures, a total of 17 elements, from nine separate fuel charges, contained worm tracks. Four of these elements were sent to Radiometallurgy Laboratory for destructive examination, to determine the mechanism of the suspected uranium cleavage.

SUMMARY AND CONCLUSIONS

During the power cycling of both April 5, 1962 and April 16, 1962, abnormal neutron flux distributions imposed severe operating conditions on the overbore fuel. The uranium alpha-beta transformation temperature (665 C) was exceeded in some of the overbore fuel cores, as a result of the high specific powers generated in the fuel columns. The reactor environment which existed at the time of the cycling--over-compensation of enriched fuel columns surrounding the block, high average exposure (~750 MWD/T) of the overbore block, and the horizontal control rod changes that are generally necessary for hot startups--were especially conducive to development of high specific powers in the overbore block.

The high specific power itself, although undesirable, may not have been the only condition which affected fuel performance. Although little is known about thermal stress in uranium, sudden changes in temperature (levels of stress) are definitely thought to be of major importance. Unfortunately, no rate of change of temperature with time data are available for these periods because the continuous coolant temperature monitoring necessary to obtain the required data is normally not provided.

Operation of the uranium at temperatures which result in the transformation from alpha to beta phase during the cycling does not represent the condition that would be expected in a full reactor loading of overbore elements. Reactor conditions in a full reactor loading of overbore elements will be different than the present environment. Upper limits of specific powers in the full reactor load of elements are expected to be about 100 Kw/ft. This is well below the levels which have been successfully maintained under present test conditions.

Studies of optimum overbore exposure, considering the elements to be perfect fuel and the present plant plutonium requirements in effect, revealed that with a full reactor loading of overbore elements, the average discharge exposure would be less than 600 MWD/T.

Eight overbore fuel elements subjected to severe cycling conditions in the reactor were selected for examination to determine the degree of damage incurred by the

DECLASSIFIED

HW-75611

Page 4

cores. Three elements had definite longitudinal worm tracks on their can walls, and one element had a suspected worm track. Four elements were used as controls, having no worm tracks. Two of the worm-tracked elements were ingot elements (74Z12, 75Z10) and the other two were dingot elements (84A1, 10A19). From the destructive examination of the incipient failures, a sequence of events has been surmized.

The three worm-track elements had longitudinal cracks in the uranium cores under the worm tracks. All three cracks were similar in shape and extended from the can wall to a point about midway to the spire then branched into a "Y" before terminating. Two of the three worm-tracked elements had areas in their cores where the alpha-to-beta transformation had occurred in the uranium. The transformed areas were crescent shaped and centered on the core tracks.

The worm tracks were shallow creases or folds in the aluminum cladding resulting from shear failure of the underlying AlSi layer at a point in line with the uranium crack. There were no deep grooves or necking in the can wall at the worm tracks that could have been caused by tension. The distinctive appearance of the worm tracks on the surface of the can wall was probably caused by the disturbance of the film along the crease. The can wall bonding had also separated extensively. The suspected worm track on dingot element 10A19 was caused from handling damage and there was no uranium core cracking.

There was no uranium cracking in any of the four elements without worm tracks although some separation of the can wall bonding had occurred. There were no differences noted in the ingot and dingot core elements.

The mechanism causing the worm tracks and the underlying core cracks can be explained by the following sequence of events:

1. Initially, radial cracks developed in the core from tensile stresses resulting when the internal uranium temperatures approached or exceeded the alpha-beta transformation temperature during the peak of a reactor cycle. The crack in the uranium propagated into the brittle compound layer at this time.
2. On the cooling cycle the core pulled away from the can wall first on one side of the crack leaving the can wall under compression.
3. Upon continued cycling, the can wall continued to separate from the core until the bond cracking reached the break across the compound layer at the end of the core crack that had formed initially.
4. At this point the progressive cracking along the bonding followed the radial crack across the compound layer into the AlSi where the AlSi failed in shear from the compressive stresses along the can wall. It was this shear crack in the AlSi layer that caused the slight offset or fold in the aluminum showing as a worm track along the surface.

5. The crack across the AlSi terminated after penetrating the aluminum a short distance. The amount of shifting along the 45° shear plane in the AlSi depended upon the magnitude of the compressive stresses and the strength of the core-to-can wall bonding. In the two elements where some alpha-beta transformation had occurred and the most severe conditions existed, there was a large offset in the AlSi and the cladding had separated from the core on both sides of the worm track. In the element in which no transformation had occurred, there was only a slight offset at the AlSi shear crack and the can wall had separated only on one side of the worm track.

GENERAL REACTOR OPERATING INFORMATION(1,2,3)

A total of 62 overbore tubes are currently installed in C Reactor--44 in a "block" near the center of the reactor, 16 located in the fringe region, and two in the lower near side of the central zone. Because of the higher uranium-to-graphite ratio of overbore columns, the effective lattice is considerably changed from the normal C lattice. The larger tubes absorb more neutrons from the surrounding area and operate at higher powers than the regular C Reactor fuel. To compensate, the central zone overbore tubes are charged with 19 pieces to limit their tube powers consistently with others in the reactor. The fringe overbore tubes have a normal length charge and do generate tube powers equivalent to regular central charges in the reactor. The 44 tube block was designed primarily to give conversion ratio data and fuel testing space. Since the block absorbs more neutrons, special enrichment is required around this block. Although tube powers can be limited by short charging, specific powers are not reduced in this manner. Thus, the specific powers have been higher than would be typical in a fully overbored reactor. The test results must, of course, be interpreted in light of these accelerated test conditions.

The first flux cycling in the time period of concern occurred on April 5, 1962. Following six days of normal operation, an unexplained Panellit scram occurred at 12:59 a.m. on April 5. A hot reactor startup was made at 1:18 a.m. During the next 12 hours of operation, a series of heat cycles took place, the latter stages of which involved tubes in the overbore block. During the cycling, temperatures were being monitored on both the Brown temperature recorder and the Flexowriter. Temperatures from a Flexowriter map run at 2:15 p.m. showed maximum tube outlet temperatures of 128 C in the top-near portion of the reactor with one overbore tube reading 127 C. At 2:45 p.m., the gamma monitor indicated the presence of fuel failure and the reactor was shut down by 3:00 p.m.

Two side-hot-spot failures were found in regular-sized tube 2955-C. Two overbore fuel columns, 2853 and 2969, were discharged and inspected, but no failures or

1. Wood, S. A., D. W. Constable, and J. R. Pierce, C Reactor Scram Recoveries, HW-73483. 4-26-62 (Secret).
2. Wood, S. A. Scram Recovery Data Preceding "C" Overbore Fuel Failures, HW-73483 SUP1. 5-15-62 (Secret).
3. Ambrose, T. W., and S. M. Graves, C Reactor Overbore Fuel Failures, HW-73580. 4-30-62 (Secret).

DECLASSIFIED

HW-75611
Page 6

failure indications were found. No additional overbore columns were discharged. A normal startup was made at 3:44 p.m. on April 7, 1962. Operation continued until April 12, when the reactor was shut down due to excessive water collection. After repairs had been made, the reactor was started up at 5:45 p.m. on April 14, 1962. At approximately 10:00 a.m. of April 16, it was decided to shut the reactor down, repair a leaky rear face connector, and attempt a hot startup. As the reactor power level was being reduced, an inadvertent scram occurred. A hot startup attempt was begun at 11:29 a.m. During this startup, no temperature maps were made, but temperatures were monitored with the Brown temperature recorder. At 11:53 a.m. the reactor was scrambled by a Panellit high trip on overbore tube 3062. The gamma monitor confirmed the presence of a failure.

Inspection of the fuel elements from tube 3062 revealed three split failures and three worm tracked pieces. On the basis of the condition of this fuel, it was decided to discharge the remainder of the tubes in the overbore block.

After discharge, all elements were visually examined and elements of special interest set aside for further study.

OVERBORE ELEMENT DATA

About 815 overbore elements were examined and a total of 20 worm tracked pieces were found. The tube numbers, element position, and uranium type of these elements are listed in Table 1. Chart 1 shows the location of the overbore tubes in the C Reactor lattice and the location of the tubes which contained worm-tracked elements.

Four of the 20 worm-tracked elements were selected for destructive examination in the Radiometallurgy Laboratory to attempt to determine the mechanism leading to the fuel failures. The four worm-tracked elements sent for examination were not selected for the apparent severity of the incipient failure, but rather for a lack of distinctness of the worm tracks. It was felt that in the attempt to deduce the sequence of events leading to fuel failure by this mechanism, the preliminary stages of failure would provide a maximum of information.

Two ingot and two dingot worm-tracked elements and two ingot and two dingot nonworm-tracked, high powered elements were selected for the examination. Pertinent operating information of the elements sent to the laboratory is contained in Table 3.

Some fuel element parameters for overbore elements were calculated using the MOFDA program and these results are listed in Table 2. The calculations show that a specific power of about 170 Kw/ft is required to cause the uranium temperature to rise to the alpha-beta transformation temperature of approximately 665 C, assuming that the heat transfer properties of the core-to-clad bond remain constant.

Chart 2 shows the results of recent non-poisonous spline flux traversing at C Reactor. It becomes apparent upon inspection of this chart, by comparing some of the observed flux peaking values with the values which would be needed to produce specific powers in excess of 170 Kw/ft, that these conditions could have existed during the more severe flux cycles.

Gamma intensity measurements (weasel) of fuel from the tubes from which elements were sent to Radiometallurgy appear in Charts 3 through 6. These charts show the average flux environment of these particular columns during their irradiation period. The shape of these curves is about typical with no major deviations from the normal. It is well to note that only minor peaking of the flux has occurred in the general region where the failures and worm-tracked elements occurred. This indicates that an abnormal flux condition would be required to give the peaking that was necessary for very high specific power. These abnormal conditions would have little effect on the weasel data if they were of short duration as is most likely to be the case for severe thermal cycling.

OVERBORE CORE HISTORY

Due to the expediency of the overbore program in late 1960, the initial quantity of overbore cores were fabricated from dingot metal by alpha extruding tubes at Weldon Springs and heat treating and machining the cores at Fernald. A second order of overbore cores fabricated from rolled ingot metal was made in late 1960 for delivery in January, 1961. The subsequent shipments of overbore cores were all fabricated from alpha extruded dingot tubes by MCW at the discretion of the AEC, since no appreciable difference in quality or preirradiation characteristics between ingot or dingot cores had been detected.

The differences in the fabrication steps between the dingot and ingot overbore cores are briefly as follows:

Dingot

1. Gamma extruded into 7" bars
2. Machined into hollow billets
3. Alpha extruded into tubes
4. Tube straightened
5. Hollow core blanked
6. Beta heat treated
7. Vacuum outgassed high H₂ metal
8. Machined to core size

Ingot

1. Cast as a 7" diameter ingot
2. Removed from No. 2 rolling stand as an oval rod
3. Rod straightened
4. Solid core blanked
5. Beta heat treated
6. Machined to core size

In the canning, the overbore cores are canned by a specially developed process. All normal quality tests and measurements are performed on the overbore pieces with an

DECLASSIFIED

HW-75611

Page 8

additional prototypic ultrasonic test for external and internal core cracks. A comparison of grain size and crack test reject rates for dingot and ingot overbore cores is as follows:

	<u>Dingot</u>	<u>Ingot</u>
UT-2 (Grain size)	2.7%	5.0%
Internal Cracks	1.5%	0.7%
External Cracks	2.3%	2.2%

Of the eight elements sent to Radiometallurgy Laboratory, specific core chemistry is known for four of the elements and the average core chemistry known for the other four pieces. The data which are available for the cores follow:

INGOT

<u>Piece #</u>	<u>Lot #</u>	<u>Ingot #</u>	<u>Density</u>	<u>Chemistry ppm</u>					
				<u>C</u>	<u>N</u>	<u>Cr</u>	<u>Fe</u>	<u>Ni</u>	<u>Si</u>
74Z12	KX010	65626	18.94	439	36	6	72	34	20
75Z8	KX010	65624	18.94	439	15	0	55	15	29
75Z9	KX010	65456	18.93	448	13	0	69	31	14
75Z10	KX010	65624	18.94	439	15	0	55	15	29
		<u>Lot Average</u>	18.936	422	17	5	72	34	20

DINGOT

<u>Piece #</u>	<u>Lot #</u>	<u>Density</u>	<u>Chemistry</u>					
			<u>N</u>	<u>Cr</u>	<u>Fe</u>	<u>Mg</u>	<u>Ni</u>	<u>Si</u>
84A10	WPO03	18.99	24	8	150	13	31	97
10A19	WPO03	<u>Lot Average</u>						
68Z9	WPO03							
68Z10	WPO03							

None of the chemistry data indicate an abnormal condition in any of the fuel cores. These cores can be said to be representative of each overbore core type.

DETAILS OF THE RADIOMETALLURGY EXAMINATION

On the elements, as received at the Radiometallurgy Building, the worm tracks were plainly discernible on two of the elements and rather faint on the third. The suspected worm track on the fourth element was obviously caused by handling damage. Crud film that accumulated during the cooling period after discharge caused the

DECLASSIFIED

HW-75611

Page 9

worm tracks to be slightly obscured. In each case the worm tracks continued in a straight line along the longitudinal axis for the entire length of the core.

On one of the nonworm-tracked elements, 75Z9, a moderate hot spot had developed on one side of the can wall. Extensive separation of the can wall bonding had occurred in this element as shown in Figure 18.

Each element was sectioned near the midpoint. In all three of the worm-tracked elements identical "Y" shaped cracks were found in the uranium cores directly under the worm tracks. On the periphery of the uranium the cracks were very fine but near the center of the core the cracks opened up and in many places were 0.003 inches wide. A typical "Y" shaped crack can be seen in the macro view in Figure 9.

In two of the worm-tracked elements, 75Z10 and 84A1, areas were found near the center of the core that had operated in the beta phase. The well-defined crescent-shaped zones are shown in the etched macro views in Figure 7 and 10. In the zones where the alpha-to-beta transformation had occurred, extensive intergranular cracking was found. These cracks, which were not continuous, were formed at the grain boundaries as a result of the severe thermal cycling stresses. When examined under high magnification, the demarcation line between the transformed and nontransformed uranium is quite distinct. In the transformed zone the recrystallized grains have distinct boundaries and numerous straight twin lines as compared to the typical hashed-up structure in the nontransformed metal. The cracks leading from the worm tracks pass through the center of these zones.

In the worm-tracked element, 74Z12, there was no indication found that the internal core temperature had reached the beta transition point. The core crack under the worm track, however, was very similar to the cracks in the other two elements. Apparently the maximum internal core temperature required to cause radial cracking of the uranium is below the beta phase transition temperature. This core was from ingot material with an average tube exposure of 708 MWD/T.

In previous investigations of worm tracks on the old solid fuel elements and some of the smaller I&E elements for split type failures, it was observed that the cladding had necked in tension when the underlying uranium had split open. On the overbore elements the worm tracks in the transverse plane appear to be slight creases or folds on the can wall surface as shown in Figures 4 and 14. The cracks in the periphery of the uranium under the worm tracks were very fine and from their appearance had not opened up previously. In this respect the mechanism that caused the worm tracks on the overbore elements is different from those observed during the examinations of other ruptured elements.

From the examination of the three worm-tracked elements it was found all had the following in common: a slight crease in the can wall surface with an underlying diagonal crack through the AlSi in line with the uranium crack. The severity of the AlSi cracking and the extent of the cladding separation from the cores varied depending upon the magnitude of the stresses in each case.

DECLASSIFIED

HW-75611

Page 10

It was during the initial heating cycle in the reactor when the interior core temperature was at a maximum that the radial cracks developed in the periphery of the core from tensile stresses. The radial cracking continued out across the brittle compound layer which must have been tightly bonded to the uranium at this time. The continuous crack from the uranium across the compound layer can be seen in Figure 15. Subsequent thermal cycles and the alternating compressive and tensile stresses in the cladding caused the bonding to separate. The concentration of stresses at the crack across the compound layer resulted in the failure of the AlSi layer and the formation of a worm track on the surface of the can wall.

In worm-tracked element 84A1, in which a transformed zone was found in the uranium core, there was a radial offset of 10 mils in the AlSi layer under the worm track. Metallographic examination of the AlSi break showed definitely that it was a shear failure as shown in Figure 6. The can wall bonding was also separated from the core on both sides of the worm track.

It would be difficult to explain how the AlSi failed in shear in line with the uranium crack in all three worm-tracked elements if it is assumed that the cladding bonding had separated on both sides of the core crack prior to the formation of the worm track. In fact, in worm-tracked element 74Z12, in which no transformation had occurred in the uranium core, the cladding had separated only on one side of the AlSi break as shown in Figures 15 and 16. The thermal cycling stresses in the cladding of this element must have been less severe than in the two worm-tracked elements where transformation had occurred because the cladding separation had not progressed beyond the worm track.

Examination of polished transverse sections from the centers of the four elements with no worm tracks failed to reveal any cracks in the uranium cores, although some separation of the can wall bonding had occurred. The macro structure of the uranium was discernible in the polished samples as shown in Figure 18, but no evidence of any transformation was found in these cores.

K.L. Hladek

Reactor Engineering
Research and Engineering Section
Irradiation Processing Department

R. Teats

Radiometallurgy Laboratory
Reactor Fuels Laboratory
Hanford Laboratories

E. Weakley

Quality and Process Control Engineering
Production Fuels Section
Irradiation Processing Department

KL Hladek: R Teats: EA Weakley: nmd

TABLE 1

Overbore Worm-Tracked Elements

<u>Tube Number</u>	<u>Fuel Series Number</u>	<u>Worm-Tracked Element Position</u>	<u>Uranium Type</u>	<u>Discharge Tube Exposure</u>
2863	63Z	9, 10, 11, 13	Dingot	714
2865	73Z	12	Ingot	670
2962	80A	9, 10, 13, 14	Dingot	712
3062*	75Z	10, 11, 13	Ingot	676
3162	84A	10	Dingot	769
3163	78A	8	Dingot	660
3169	74Z	12	Ingot	708
3367	7A	17	Dingot	522
3262	10A	19	Dingot	578

* Tube 3062 contained the failed elements.

TABLE 2

Calculated Overbore Fuel Conditions

<u>Tube Power</u> Kw	<u>Specific Power</u> Kw/ft	<u>Maximum Elastic Stress</u> psi	<u>Maximum Uranium Temperature</u> °C
19 element column			
1435	109	113,300	462
1636	124	125,600	515
1830	139	135,500	566
2030	155	142,000	616
2230	170	144,100	665
32 element column			
1000	60	62,500	272
1200	72	74,300	318
1400	84	85,500	365
1600	96	96,400	406

TABLE 3

Overbore Element
Operating Conditions
April 4 - April 16

<u>Tube</u>	<u>Elements</u>	<u>Charge Date</u>	<u>Average Tube Flow</u> gpm	<u>Average Tube Power</u> Kw	<u>Discharge Tube Exposure</u> MWD/T	<u>Maximum Tube Outlet Temperature</u> °C	<u>Maximum¹ Tube Power</u> Kw	<u>Maximum² Specific Power</u> Kw/ft	<u>Average Tube Outlet Temperature</u> °C	<u>Average³ Specific Power</u> Kw/ft	<u>Number of⁴ Observed Cycles</u>	<u>Per cent⁵ Peaking Required</u>
3162	84A10	12-8-61	58	1450	769	127	1820	145	102	86	4	17
3062	75Z8 75Z9 75Z10	12-8-61	59	1300	676	114	1654	133	92	78	2	28
3169	74Z12	12-8-61	57	1300	708	117	1635	131	93	78	0	30
3262	10A19	1-16-62	58	1450	578	124	1775	142	102	86	4	20
2969	68Z9 68Z10	12-8-61	58	1350	594	114	1590	127	97	80	0	34

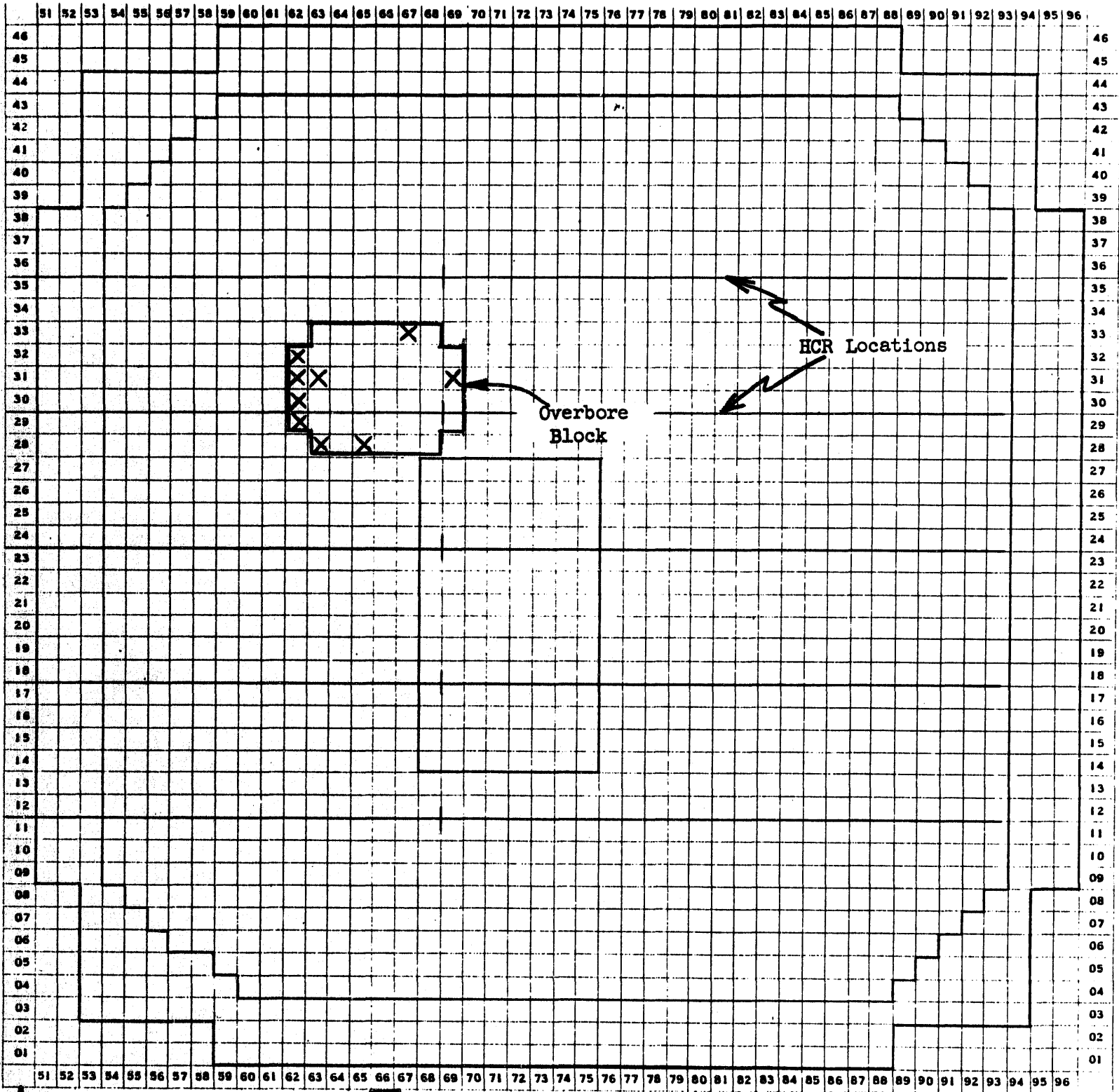
1. Maximum tube power observed during these periods of flux cycling.
2. Maximum specific power observed during the cycling, assuming a cosine flux distribution.
3. Normal maximum specific power for the complete irradiation period, assuming a cosine flux distribution.
4. Cycle defined as a tube outlet temperature change of greater than 10 C within a 30 minute time period.
5. The per cent flux peaking over cosine, with the maximum observed tube power, to obtain a maximum specific power of 170 Kw/ft.

DECLASSIFIED

DECLASSIFIED

CHART 1

Front Face Map - C Reactor



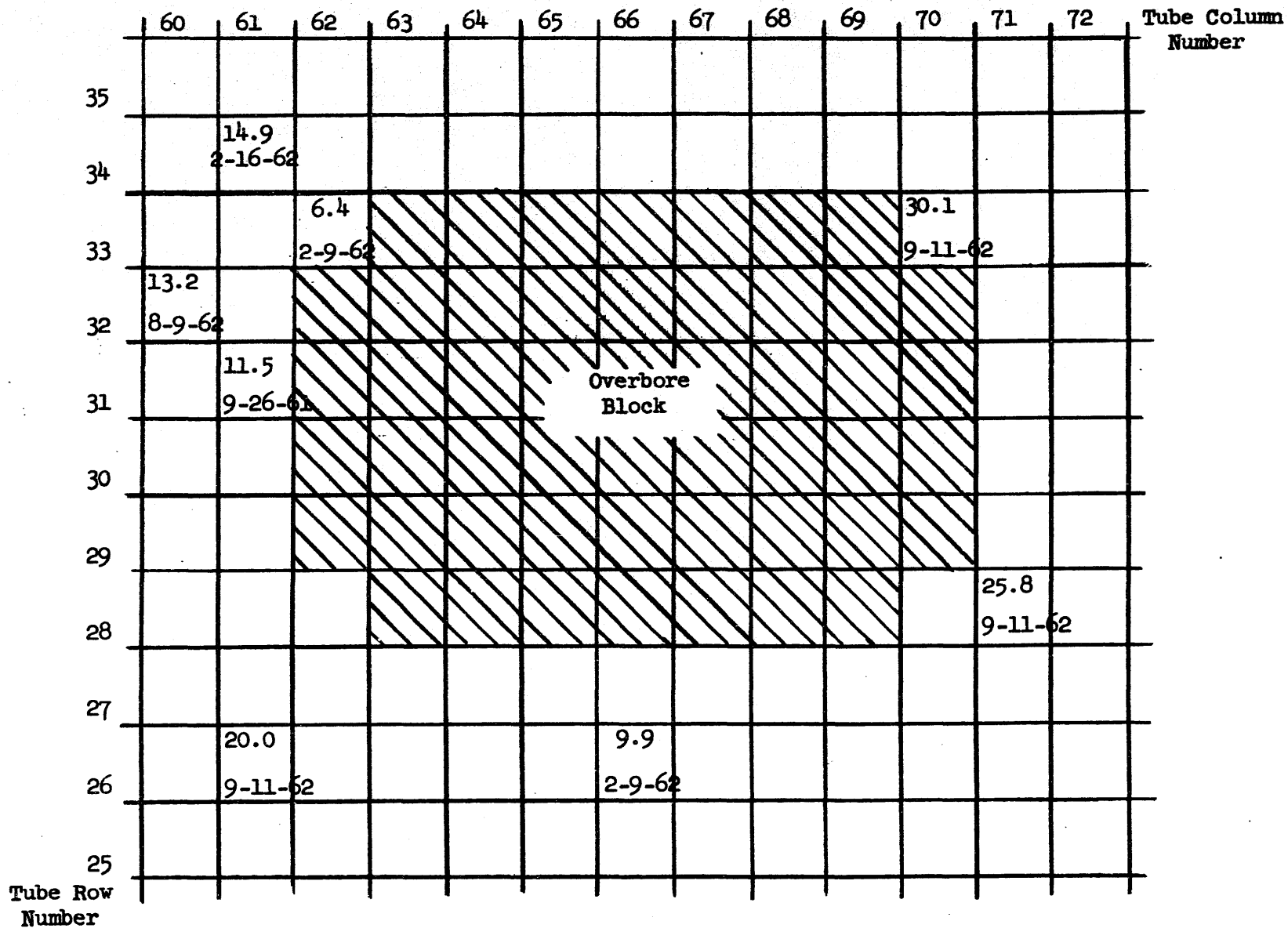
Tube Row Number

Tube Column Number

"X" indicates overbore tube location which contained worm-tracked elements.

CHART 2

Nonpoisonous Spline Flux Traverse Results - C Reactor

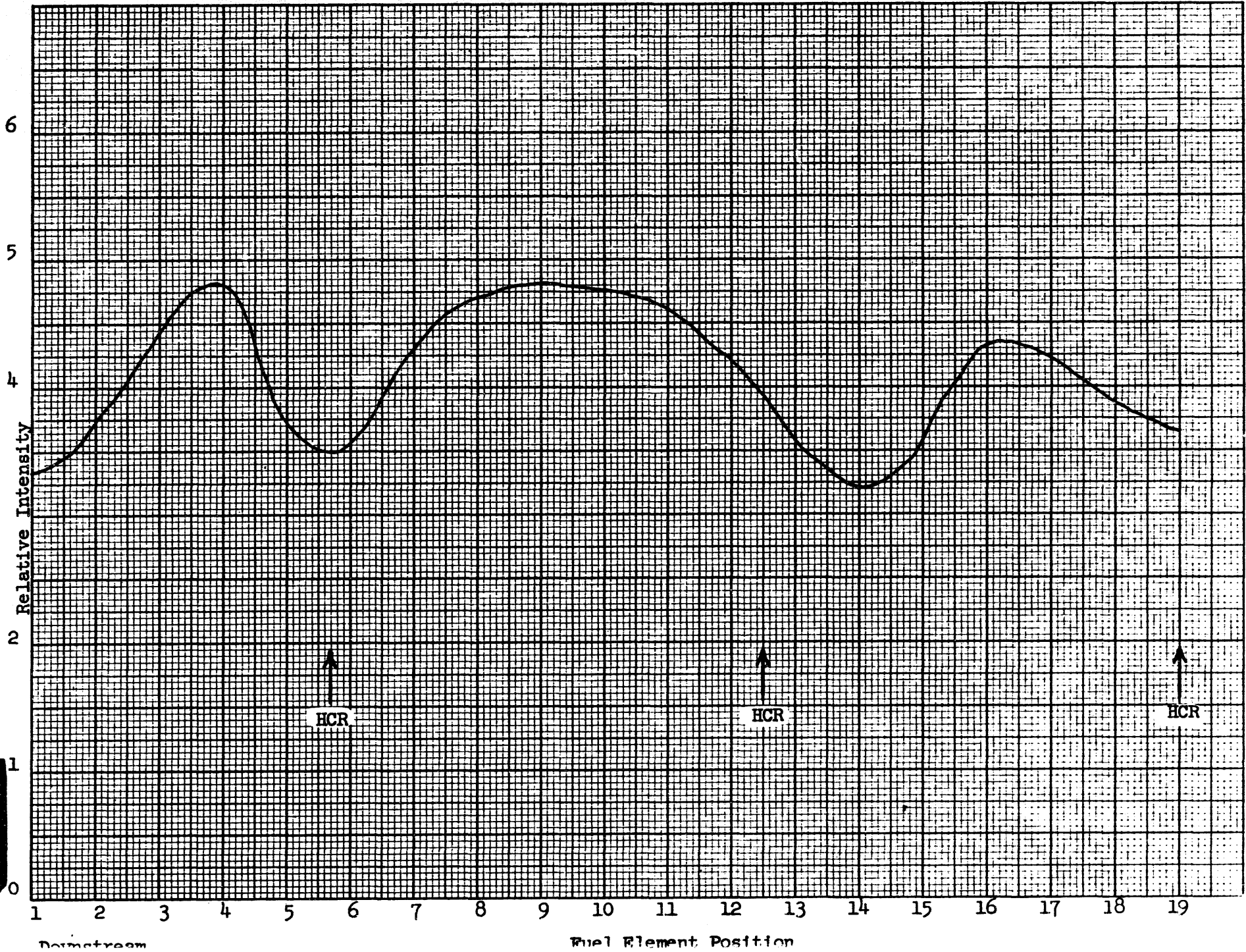


Data show traverse locations, per cent flux peaking over cosine value, and date of traverse.

DECLASSIFIED

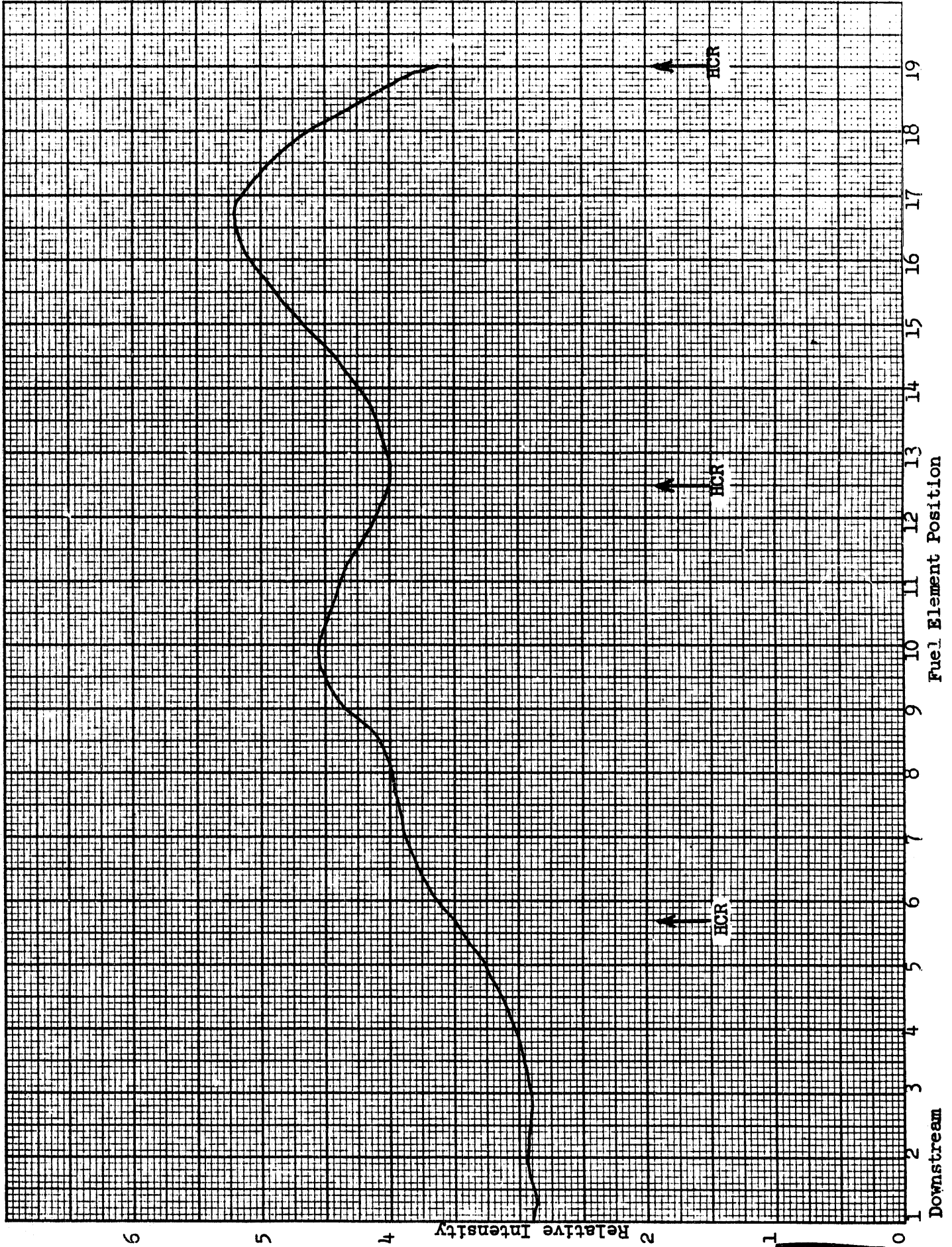
Gamma Intensity Measurements
Overbore Fuel Column 3062-C
Discharged 4-16-62

PR-84(1-62) ACAS RECORD, VASA

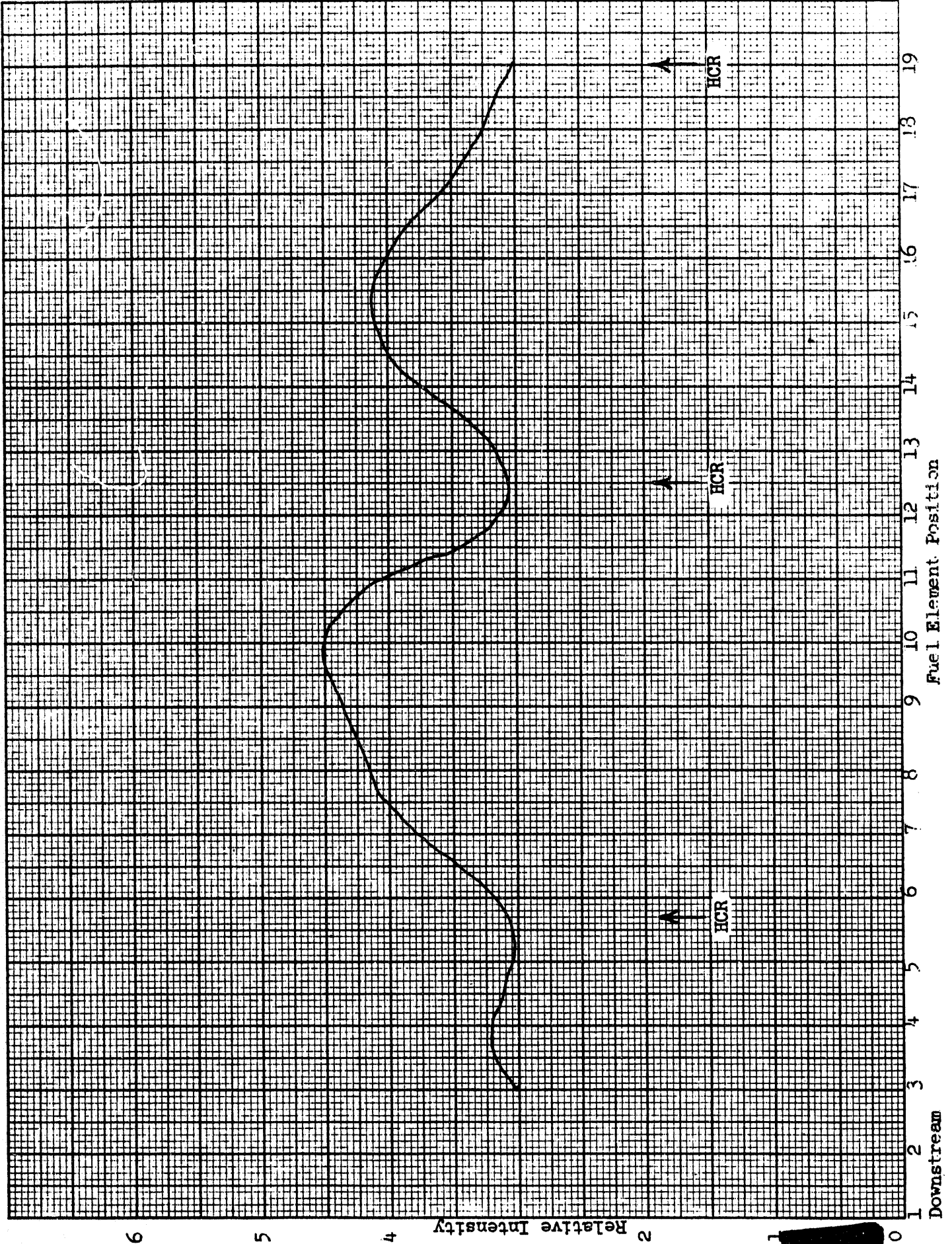


DECLASSIFIED

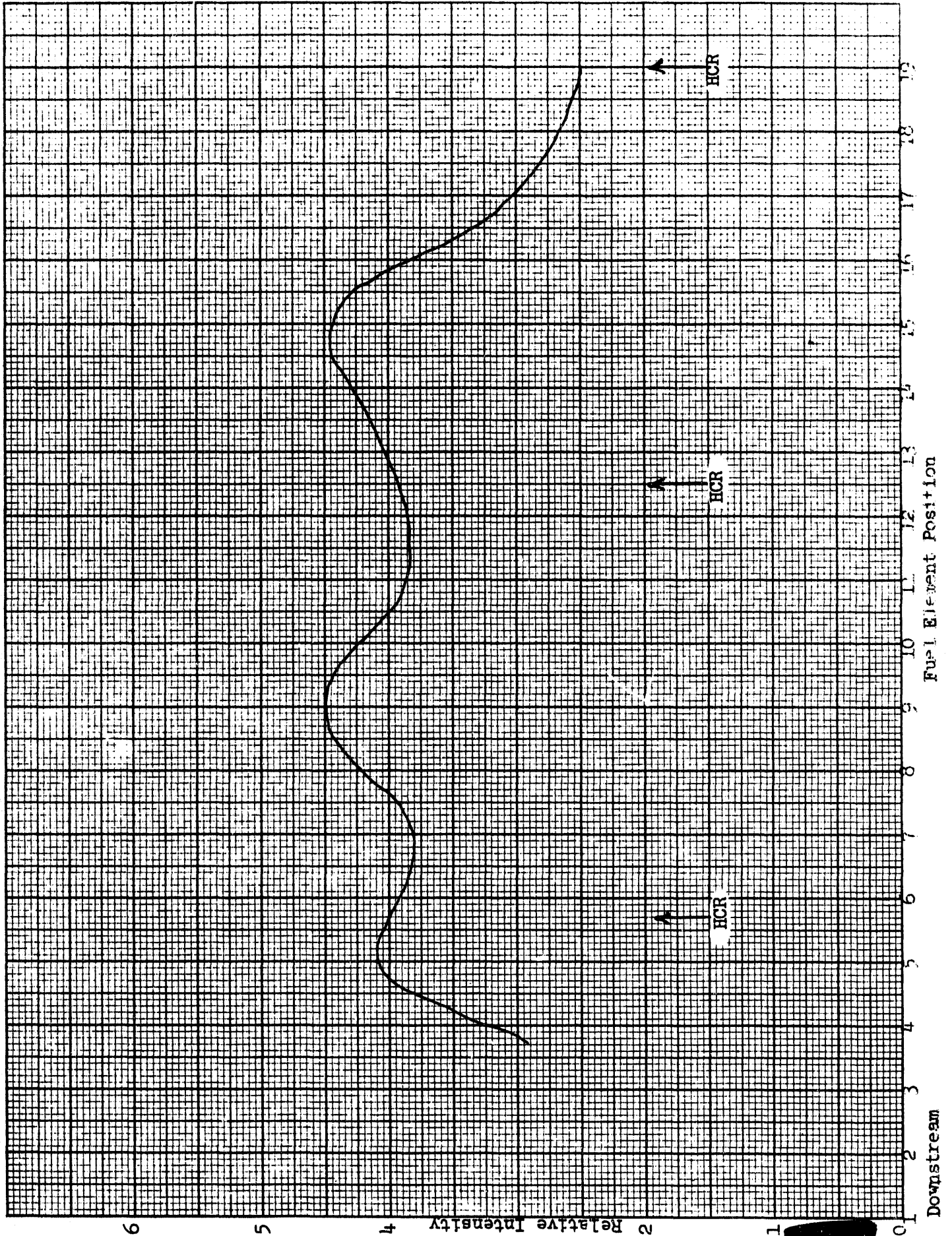
Gamma Intensity Measurements
Overbore Fuel Column 3262-C
Discharged 4-16-62



Gamma Intensity Measurements
Overbore Fuel Column 2969-C
Discharged 4-16-62



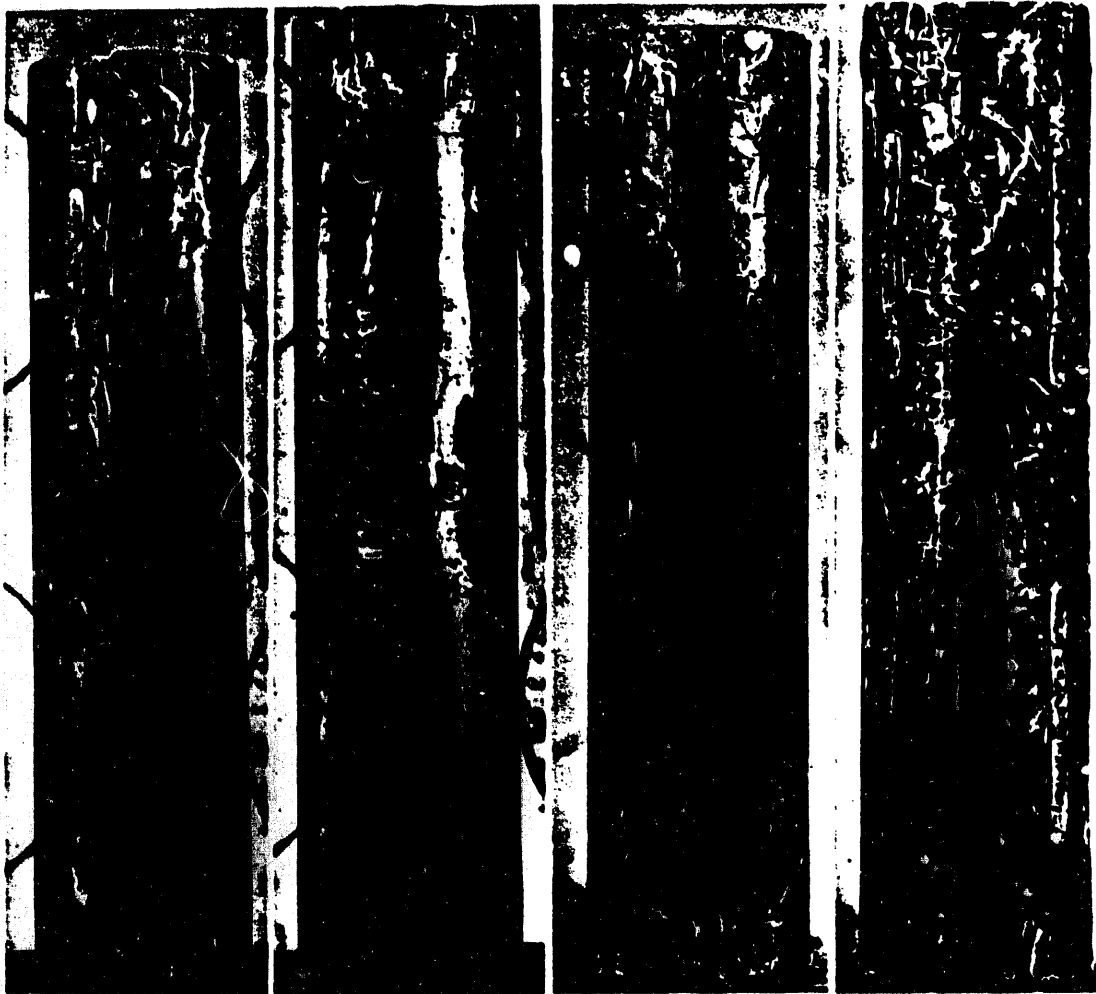
Gamma Intensity Measurements
Overboard Fuel Column 3169-C
Discharged 4-16-62





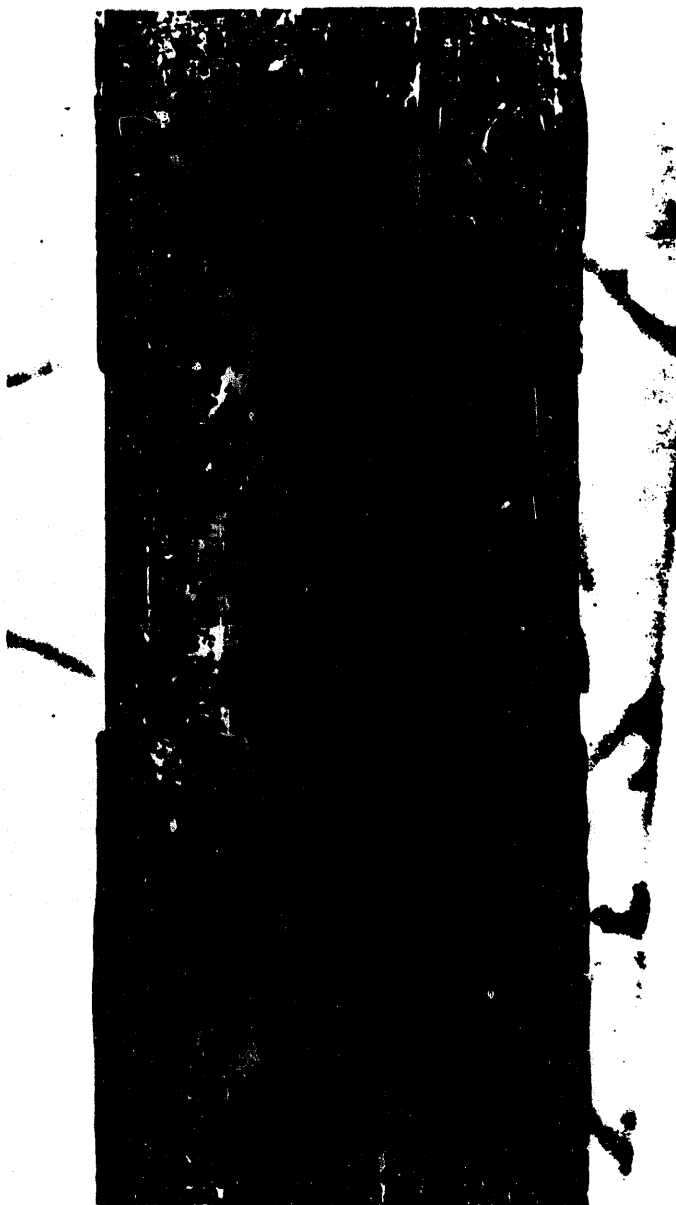
Neg. #	B1588	B1591	B1554	B1558	.5X
Element	75Z10	74Z12	84A1	10A19	
Tube	3062C	3169C	3162C	3262C	
Core	Ingot	Ingot	Dingot	Dingot	

Figure 1 - As-received views showing three worm track elements and suspected worm track in Neg. # B1558.



Neg. #	B1579	B1569	B1538	B1544	.5X
Element	75Z8	75Z9	68Z10	68Z9	
Tube	3062C	3062C	2969C	2969C	
Core	Ingot	Ingot	Dingot	Dingot	

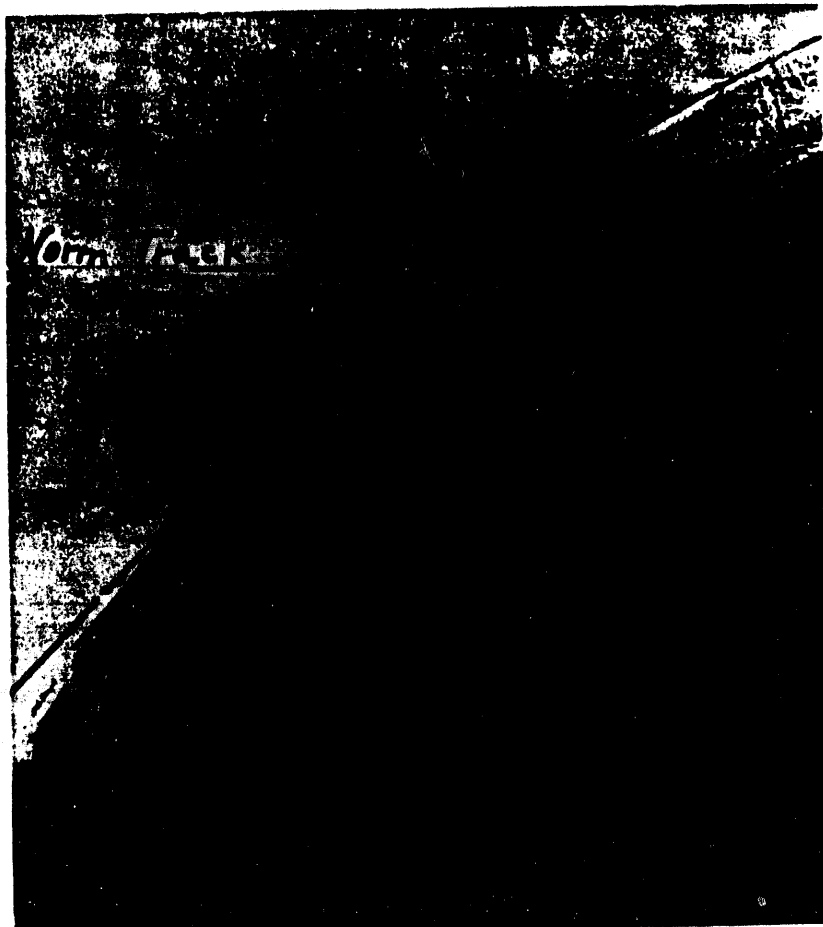
Figure 2 - As-received views of four elements with no worm tracks.



Neg. # B1595

1.3X

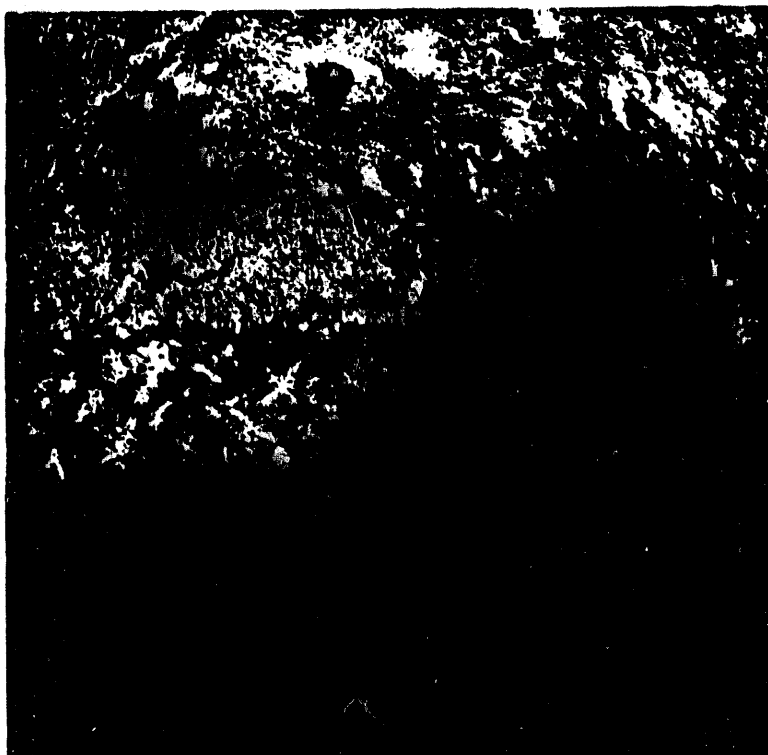
Figure 3 - Close-up view of worm track on Element 74Z12.



Neg. # B1994

10X

Figure 4 - Transverse section through worm track on Element 84Al showing core crack, off-set in AlSi and contour of worm track. A small piece of fractured AlSi had fallen out of the AlSi break in this view and the break appears wider than it was. Higher magnification views are shown in Figures 5 and 6.

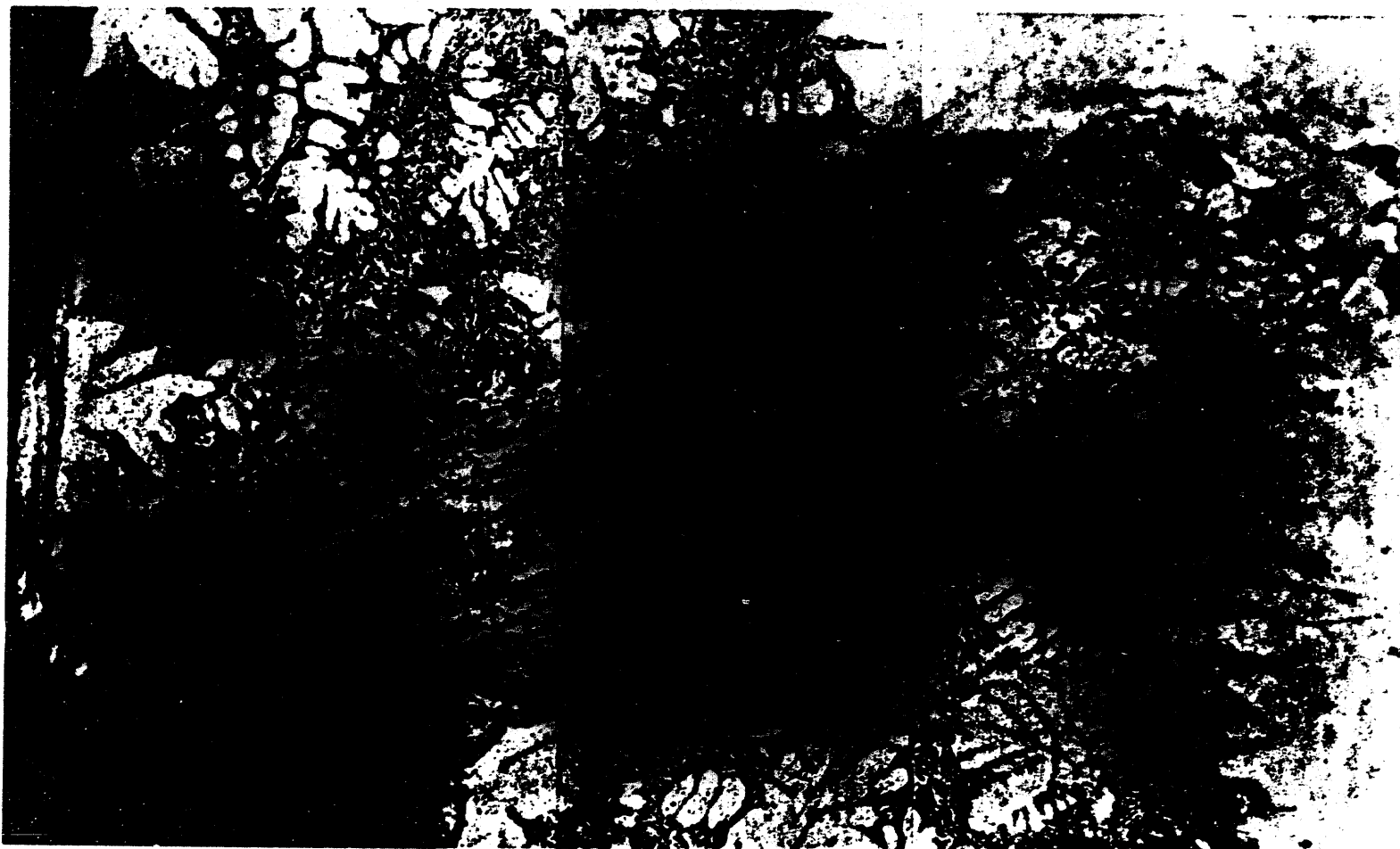


Neg. # B1995

60X

Figure 5 - Transverse section of Element 84A1 showing core crack and shear break in AlSi.

PHOTOGRAPHS UNCLASSIFIED



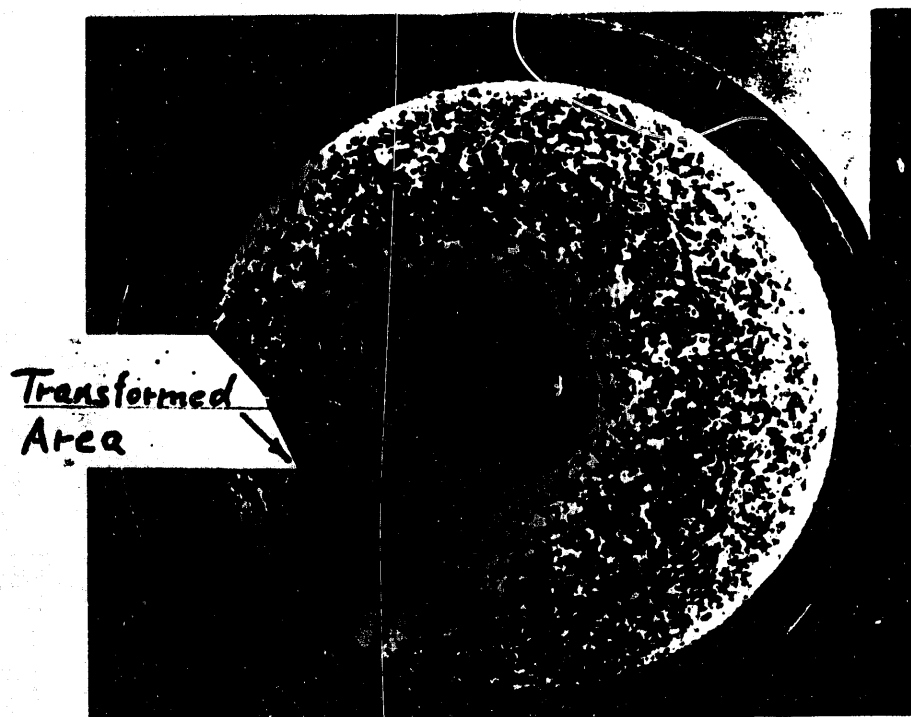
Neg. # B2000

300X

Figure 6 - Enlarged view of break in AlSi of Element 84A1 showing shear flow lines.

PHOTOGRAPHS UNCLASSIFIED

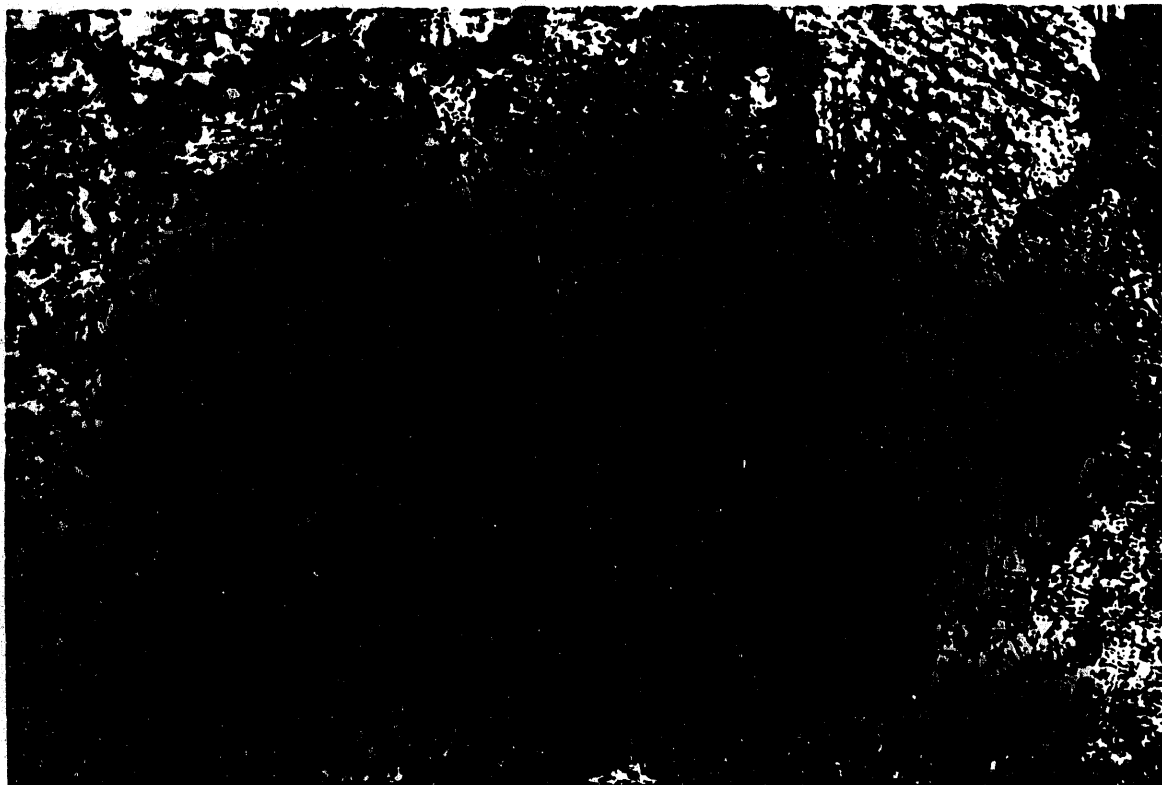
HM-75611



Neg. # B2257

2X

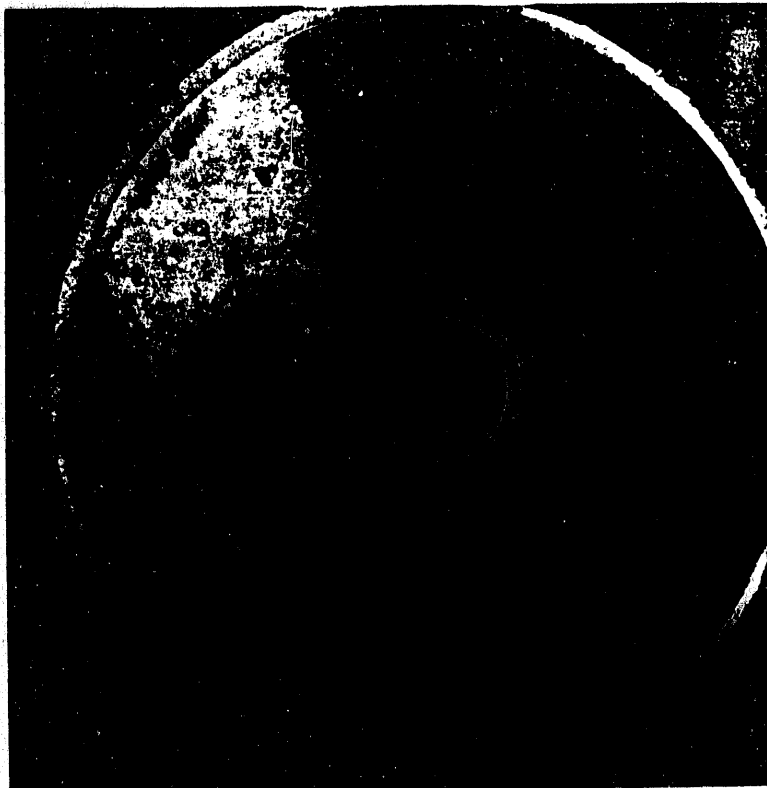
Figure 7 - As-etched section from worm track Element 84A1 showing small transformed area in core and Y-shaped crack at lower left.



Neg. # B2311

75X

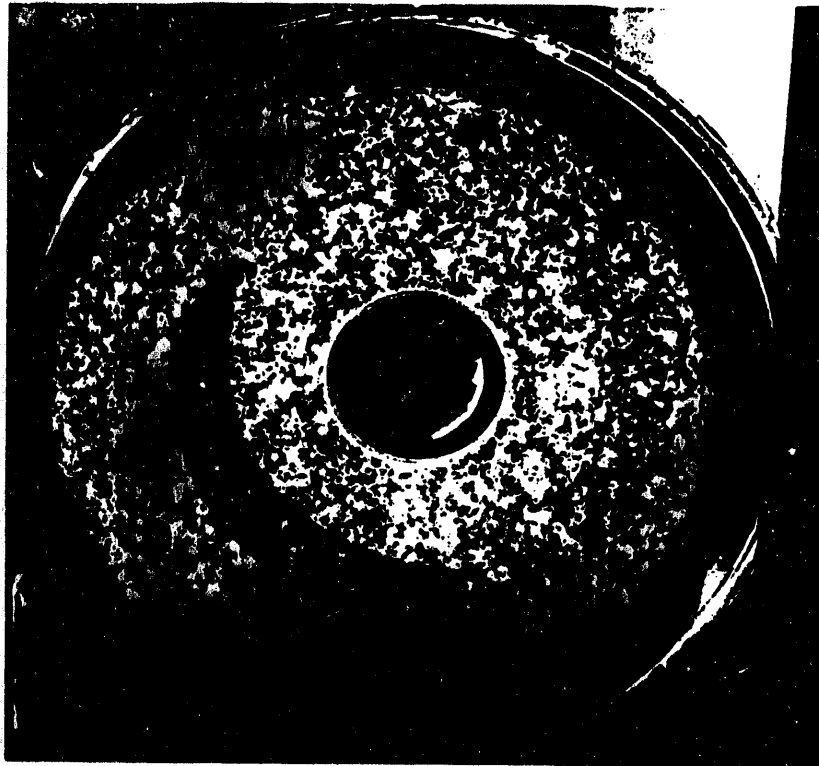
Figure 8 - Transverse section from Element 84A1 showing edge of transformation zone in uranium core. The transformed area is shown in the upper right half of photo.



Neg. # B2005

2X

Figure 9 - Transverse section as-polished through worm track element showing typical Y-shaped crack in uranium core.



Neg. # B2260

2X

Figure 10 - As-etched transverse section from worm track Element 75Z10 showing crescent-shaped zone where the uranium had operated in the beta phase.



Neg. # B2275

75X

Figure 12 - Grain boundary cracking of uranium in the transformed zone of worm track Element 75Z10.



Neg. " D27/12

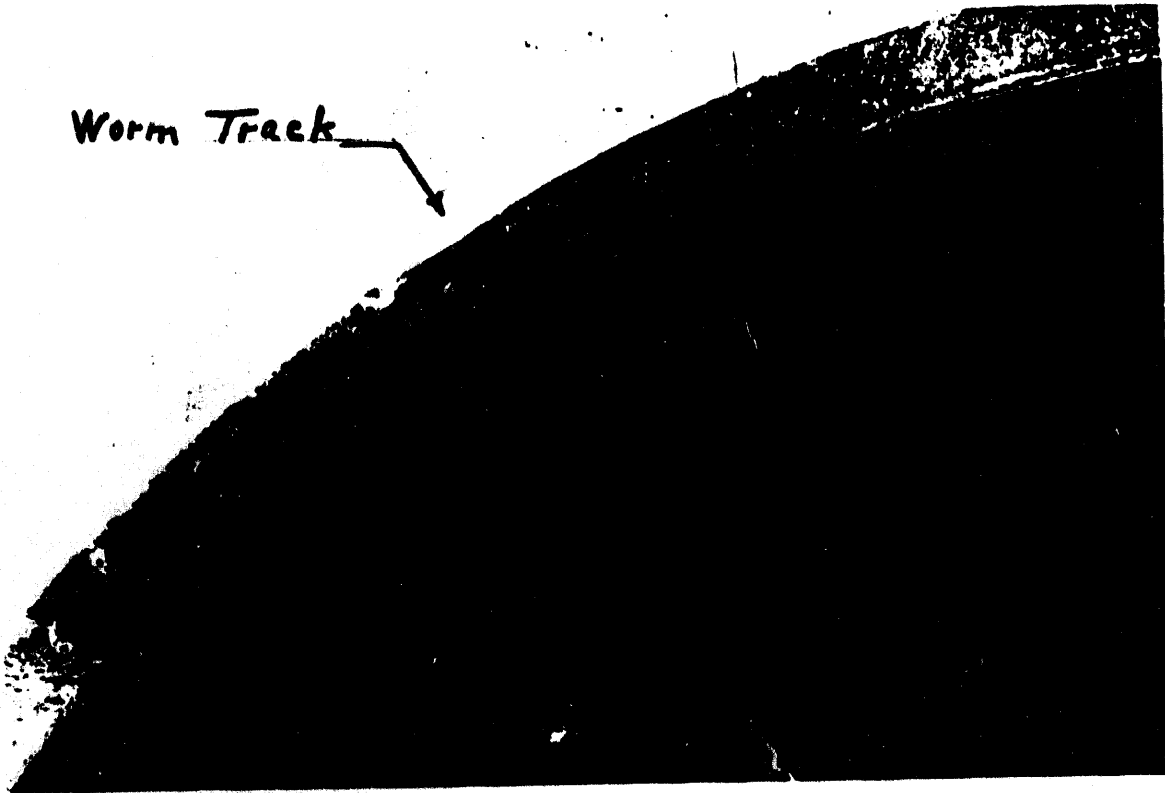
As-Polished

Neg. " D2338

As-Etched

2X

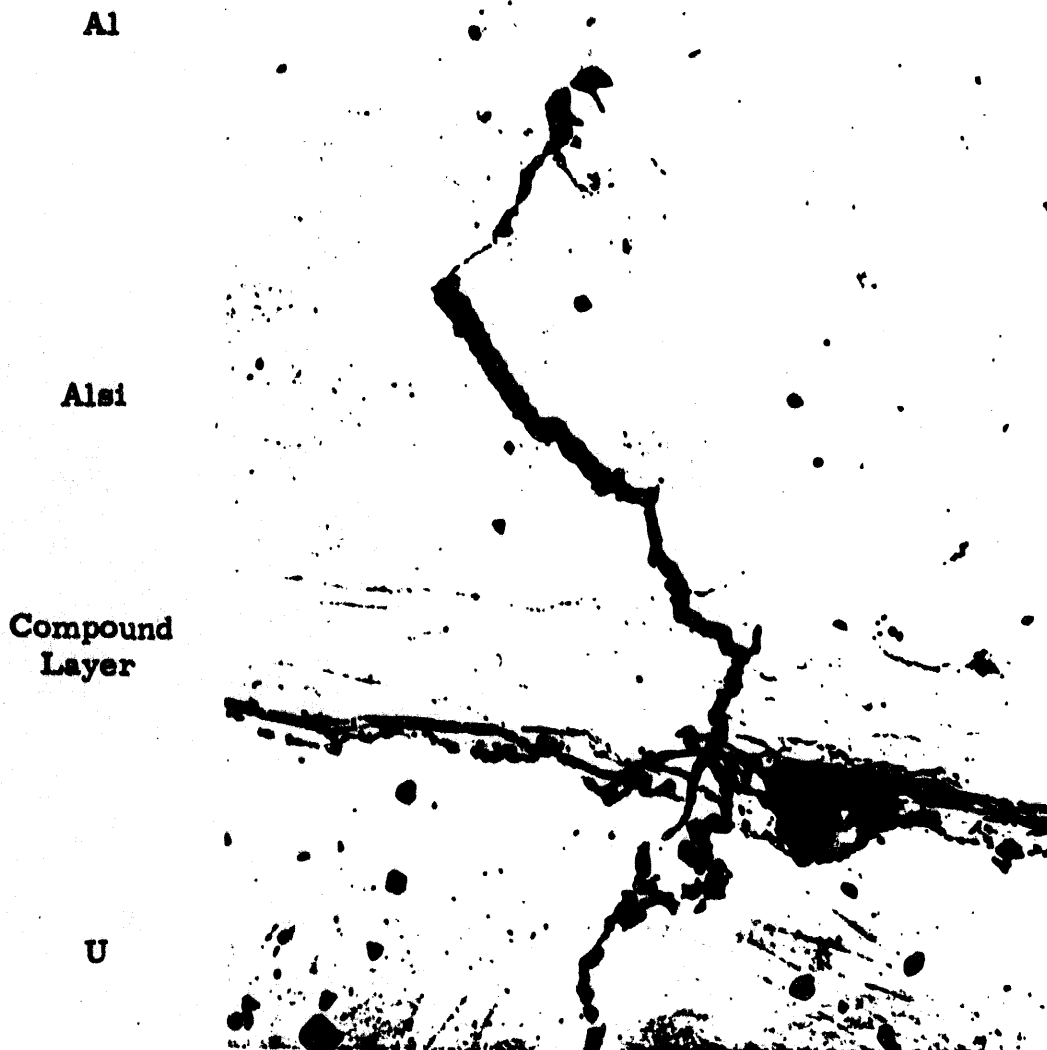
Figure 13 - Transverse section as-polished and as-etched of 74Zl2. The worm track is at the top but not visible in these views. Part of the core crack can be seen at the top of the as-polished section. Note the cladding separation at 60° from the crack. No evidence of transformation was found in this core.



Neg. # B2850

10X

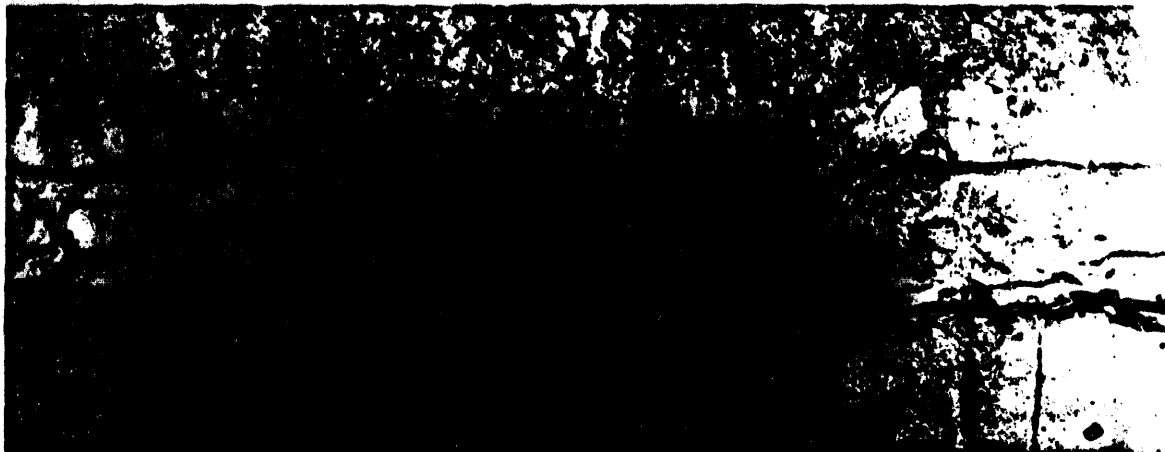
Figure 14 - Transverse section through worm track on Element 74Z12 showing core crack and contour of worm track. Note cladding separation at right of crack.



Neg. # B2827

250X

Figure 15 - Transverse section from 74Z12 showing crack continuing from uranium at bottom through compound layer and then across AlSi. Separation at uranium interface continues for more than 90° at the right of crack but at the left the separation terminates at .030" from crack.

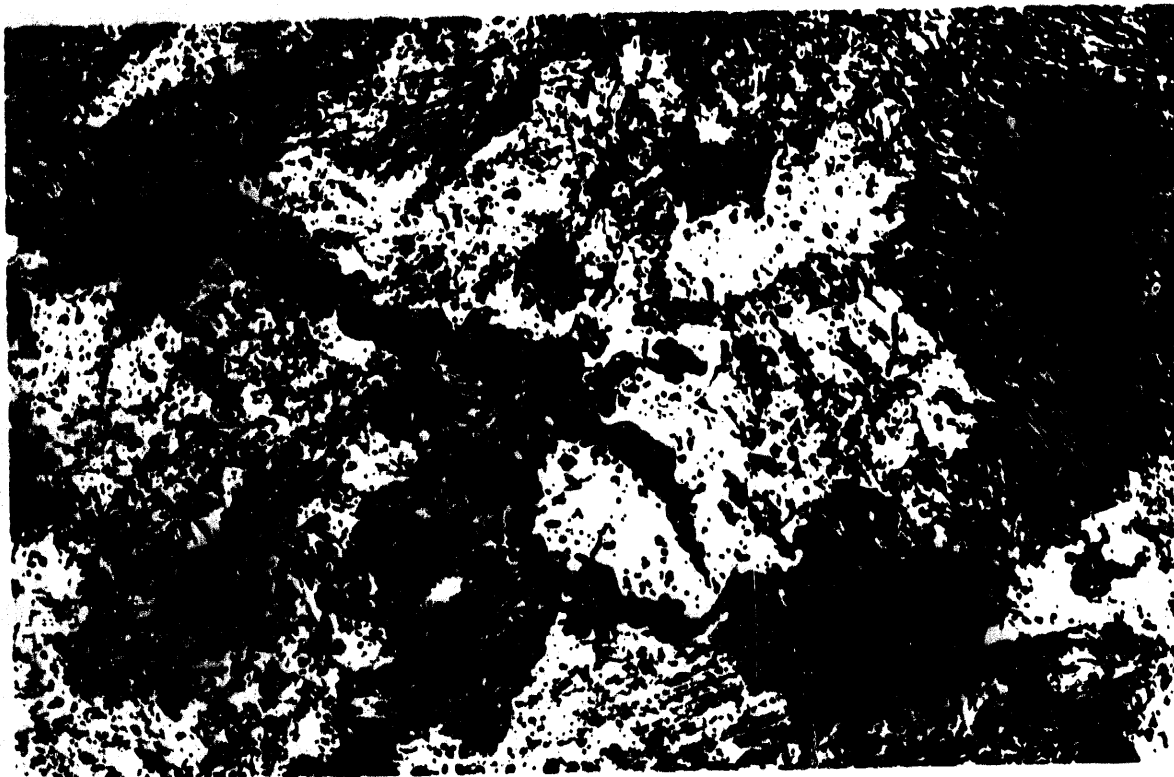


Neg. # B2824 and B2826

250X

Figure 16 - View at top shows end of bonding separation at .030" from left of uranium crack shown in Figure 15.

View at bottom is bonding separation at right of uranium crack and shows fragmented edges from cycling stresses.



Neg. # B2256

75X

Figure 17 - Transverse section showing cracking along uranium grain boundaries near the center of core from 74Z12. This element had a worm track in the cladding and a cracked core but no evidence was found that it had operated in the beta phase.



Neg. # B2985

Neg. # B2999

2X

Figure 18 - As-polished sections from 75Z9 on left and 68Z10 showing macro structure of uranium. These elements had no worm tracks or uranium cracking. The extensive canwall bonding separation can be seen on the bottom of 75Z9.

DATE
FILMED

8/4/94

END

